ELSEVIER

www.elsevier.nl/locate/jorganchem

Journal of Organometallic Chemistry 603 (2000) 203–212

Journal of Organometallic Chemistry

Preparation, crystal structure determination and properties of adducts of indium methylene compounds with Group 15 donors

L. de Araújo Felix [a], C.A.F. de Oliveira [a], R.K. Kross [a], C. Peppe [a], M.A. Brown [b], D.G. Tuck [b,*], M.Z. Hernandes [c], E. Longo [c], F.R. Sensato [c]

[a] *Departamento de Quimica, CCEN, Universidade Federal da Paraiba, Campus I, 58.059-900 João Pessoa-PB, Brazil*
[b] *Department of Chemistry and Biochemistry, University of Windsor, Windsor, Ont., Canada, N9B 3P4*
[c] *Departamento de Quimica, Universidade Federal de São Carlos, São Carlos-SP, Brazil*

Received 17 September 1999; received in revised form 2 February 2000

Abstract

The reaction of InBr with CH_2Br_2 in 1,4-dioxane or acetonitrile yields the corresponding solvate of Br_2InCH_2Br, which on reaction with $E(C_6H_5)_3$ ($E = P$, As, Sb) gives the indium(III)-Group 15 dimetallo-methane derivatives, $Br_3InCH_2E(C_6H_5)_3$. The crystal structures of the two related compounds ($E = As$, Sb) have been determined by X-ray crystallography. For $Br_3InCH_2As(C_6H_5)_3$, cell constants $a = 15.553(7)$, $b = 21.646(8)$, $c = 12.920$ (10) Å; space group *Pbca*, $Z = 8$, $R = 0.064$, $R_w = 0.054$, and for $Br_3InCH_2Sb(C_6H_5)_3$, $a = 15.439(6)$ Å, $b = 22.016(4)$ $c = 13.138(5)$ Å; space group *Pbca*, $Z = 8$, $R = 0.062$, $R_w = 0.049$. Results are also reported for $I_3InCH_2As(C_6H_5)_3$ (cell constants $a = 12.0122(2)$, $b = 15.8526(3)$, $c = 13.4180(3)$ Å, $\beta = 109.933(1)°$; space group $P2_{1/n}$, $Z = 4$, $R = 0.0481$, $R_w = 0.0431$) and $Br_3InCH_2N(C_2H_5)_3$ ($a = 7.362(2)$, $b = 14.700(2)$, $c = 13.049(1)$ Å, $\beta = 98.90(1)°$; space group $P2_{1/n}$, $Z = 4$, $R = 0.0418$, $R_w = 0.0368$). The structural results are compared with those for other organoindium ylids with the same general structure Br_3InCH_2L ($L = P(C_6H_5)_3$; 1,1,3,3,-tetramethyl-2-thiourea; *N*,*N*,*N*′,*N*′-tetramethylethanediamine). Semi-empirical quantum mechanical calculations, using the PM3 method, were carried out on the series $Br_3InCH_2E(C_6H_5)_3$ ($E = P$, As, Sb), and the calculated structural parameters are compared with the values determined by X-ray crystallography. The presence of an ylid ligand $H_2C^{\delta-}\text{—}^{\delta+}E(C_6H_5)_3$ in the organoindium compounds is confirmed. Mass spectra and thermogravimetric analysis strongly suggest that the thermal decomposition of the compounds occurs via fission of the indium–carbon bond, leading to the corresponding ylid, which can be trapped by reacting the $X_3InCH_2E(C_6H_5)_3$ compounds with HBr to produce the onium derivative $[CH_3E(C_6H_5)_3]^+$ $[InX_4]^-$ ($E = P$, As; $X = Br$, I). © 2000 Elsevier Science S.A. All rights reserved.

Keywords: Crystal structure determination; Indium methylene compounds; Group 15 donors

---

1. Introduction

For some years, interest in the organometallic compounds of indium was related to their use in semiconductors, but the recent literature [1,2] has shown that interesting organic transformations, such as the cyclopropanation of electron-deficient alkenes and the epoxidation of carbonyl compounds, can be achieved by reaction with indium metal and dialkyldihalides. The preparation of indium(III) compounds [3–6] of general structure $X_2InCR^1R^2X$ ($R^1 = H$; $R^2 = H$, halogen, alkyl) has allowed the study of the properties of these complexes, which may function as carbene transfer reagents. It has been argued elsewhere that the chemistry of such molecules is associated with the tautomeric structure IB arising from intramolecular halide transfer from the carbon atom to the metal center (Scheme 1) to give a species in which the carbon atom is highly electron deficient. This description predicts that α-halogeno-alkylindium(III) compounds will have two sites available for electron pair donation, namely the indium atom and the halogenomethylic carbon. In agreement with this, we have shown that the addition of halide anion to $X_2InCHRX$ ($R = H$), leads to the corresponding salts of $[X_3InCHRX]^-$ ($X = Cl$, Br, I],

---

* Corresponding author. Fax: + 1-519-9737098.
E-mail address: dgtuck@uwindsor.ca (D.G. Tuck)

PII: S0022-328X(00)00178-9

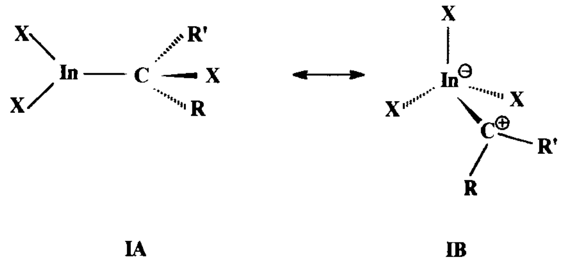

Scheme 1.

and the crystal structures of such anions (X = Cl, Br) have been established recently by X-ray methods. We have also synthesized adducts derived directly from structure IB, with the ligand attached directly to the carbon atom, including the compounds $Br_3InCH_2P(C_6H_5)_3$, $Br_3InCH_2N(Me)_2CH_2CH_2NMe_2$ and $Br_3InCH_2SC(NMe_2)_2$, and these have also been characterised fully [3–9].

We have now extended this latter part of the work by preparing and structurally characterising adducts of Br_2InCH_2Br with triethylamine, triphenylarsenic and triphenylantimony, and of triphenylarsenic and I_2InCH_2I. In each case the product is the appropriate $X_3InCH_2ER_3$ compound (E = N, As, Sb). The structural and thermal properties of these species are discussed in the light of model calculations on the bromo compounds.

2. Experimental

2.1. General

Indium monobromide was prepared by heating metal and trihalide together in a sealed tube at 450°C. Methylene bromide (Aldrich) was dried over Linde 4A molecular sieves. Triphenylarsenic and antimony (Aldrich) were used as supplied. 1,4-Dioxane and tetrahydrofuran were dried over sodium and benzophenone, and distilled just before use from the blue ketyl form. Acetonitrile was dried over CaH_2, and distilled before use. Methylene chloride, diethyl ether, acetone and ethanol (95%) were ACS grade (Merck) and were used as supplied.

Indium analysis was by back-titration of excess EDTA with thorium nitrate, and bromide analysis by the Volhard method, as described previously [8]. Microanalysis was by Canadian Microanalytical Services Ltd. Proton and carbon-NMR spectra were recorded on a Bruker AC300L spectrometer. Thermogravimetric analysis was carried out on a Shimadzu TGA-50 instrument, under a nitrogen atmosphere (flow rate 20 ml min^{-1}); the sample (ca. 10 mg) contained in an alumina cell, was heated over the range 30–800°C at a constant rate of 10°C min^{-1}. Mass spectra were recorded on a Hewlett Packard 5890-II spectrometer operating in the E.I. mode.

All preparative work was conducted under dry nitrogen, using standard vacuum line techniques, up to the isolation of the $Br_3InCH_2ER_3$ compounds, which are air stable.

2.2. Preparative

2.2.1. $Br_3InCH_2N(C_2H_5)_3$

InBr (0.58 g, 2.95 mmol) and CH_2Br_2 (0.63 ml, 1.56 g, 9 mmol) were stirred together in acetonitrile (20 ml) to dissolution of InBr; at this point all the volatiles were removed under vacuum to ensure absence of excess CH_2Br_2. The oil obtained was redissolved in acetonitrile (20 ml) and to this solution was added $N(C_2H_5)_3$ (0.41 ml, 0.30 g, 2.95 mmol). The reaction mixture was stirred for 12 h, at which point the powder that precipitated was collected by filtration and discarded. The solution was concentrated under vacuo to 1/3 of its initial volume and ethanol (95%; 8 ml) added; slow evaporation of the solution (open to the air) lead to precipitation of $Br_3InCH_2N(C_2H_5)_3$ (0.51 g, 1.10 mmol, 37%) as colorless single crystals. Anal. Found: C, 18.1; H, 3.74; N, 2.98; In, 24.0; Br, 50.2; Calc. for $C_7H_{17}NInBr_3$ C, 17.9; H, 3.65; N, 2.98; In, 24.4; Br, 51.0. ^1H-NMR (acetone-*d*6); 1.45, t, 9H (NCH_2CH_3); 3.20, s, 2H ($InCH_2$); 3.55, q, 6H (NCH_2CH_3) (all in ppm, $Me_4Si = 0$). ^{13}C-NMR; 9.23 (NCH_2CH_3); 59.03 (NCH_2CH_3) ppm ($Me_4Si = 0$). $InCH_2$ was not detected.

An analogous experiment with equimolar quantities of Br_2InCH_2Br and $N(C_6H_5)_3$ in acetonitrile involved stirring for 12 h at room temperature (r.t.), followed by refluxing for 1 h. Evaporation of volatile components gave a white solid, from which 67% of the initial $N(C_6H_5)_3$ was recovered. There was no evidence of adduct formation.

2.2.2. $Br_3InCH_2E(C_6H_5)_3$

InBr (0.50 g, 2.56 mmol) was suspended in 1,4-dioxane (20 ml), and CH_2Br_2 (1.0 ml, 2.48 g, 14.2 mmol) added via a syringe. The reaction mixture was stirred until the monobromide dissolved (ca. 3–4 h). All the volatiles were removed under vacuum, and the mixture kept under vacuum to ensure complete removal of excess CH_2Br_2. This led to the formation of the bisdioxane adduct of $BrInCH_2Br$, which was redissolved in dioxane (20 ml). Solid $E(C_6H_5)_3$ (E = As, 0.78 g, 2.56 mmol; E = Sb, 0.90 g, 2.56 mmol) was added to the solution, and the reaction mixture stirred for 6 h to yield a colorless solution from which the individual compounds were isolated according to the following procedures.

2.2.2.1. $Br_3InCH_2As(C_6H_5)_3$. The solution from the reaction was filtered to remove small amounts of solid residue, and solvent removed partially under vacuum to the onset of crystallisation; on standing, complete precipitation occurred, giving $Br_3InCH_2As(C_6H_5)_3$ (1.40 g, 2.07 mmol, 81%) as cubic crystals, which were dried in vacuo. Under vacuum, the crystallinity was lost to give an amorphous white solid, and the analytical results, and the NMR spectra, are for this latter material. Suitable single crystals for X-ray analysis were grown by dissolving the compound in dichloromethane and reprecipitating by the slow addition of diethyl ether in a closed vessel. Anal. Found: In, 17.5; Br, 35.5; Calc. for $C_{19}H_{17}AsBr_3In$; In, 17.0; Br, 35.5. ^{1}H-NMR (acetone-*d*6) 7.7–7.1, m, 15H (C_6H_5) 2.21, s, 2H(In–CH_2). ^{13}C 134.51, 133.80, 132.18, 131.15, 130.62, (C_6H_5) 9.58 ($InCH_2$) ppm.

2.2.2.2. $Br_3InCH_2Sb(C_6H_5)_3$. All the volatiles from the reaction solution were removed under vacuum to leave a colorless oil; addition of toluene (10 ml) caused the precipitation of a white solid, which was filtered in vacuo, and recrystallised in 1:1 v/v acetone–ethanol (95%, 20 ml) to yield crystals of $Br_3InCH_2Sb(C_6H_5)_3$ suitable for X-ray analysis (1.20 g, 1.66 mmol, 65.0%). Anal. Found: C, 31.8; H, 2.44; In, 15.4; Br, 33.5; Calc. for $C_{19}H_{17}SbBr_3In$; C, 31.6; H, 2.38; In, 15.9; Br, 33.2.

2.2.3. $I_3InCH_2As(C_6H_5)_3$

InI (0.30 g, 1.23 mmol) and CH_2I_2 (0.10 ml, 0.33 g, 1.23 mmol) were stirred together in THF (20 ml) at 0°C to complete dissolution of InI; $AsPh_3$ (0.3 g, 1.23 mmol) was added and the mixture stirred for 2 h. Volatiles were removed under high vacuo to give an oil which was recrystalized in acetone–ethanol (25 ml, 1:1, v/v) yielding $I_3InCH_2AsPh_3$ (0.75 g, 0.92 mmol, 75%) as colorless single crystals. Anal. Found: In, 13.6; I, 46.9; Calc. for $C_{19}H_{17}$ $AsInI_3$; In, 14.1; I, 46.7. ^{1}H-NMR (acetone-*d*6): 2.45 s, 2H (In*CH*$_2$As), 7.61–7.71m, 15h (As*Ph*$_3$) ^{13}C-NMR: 7.87 (In*CH*$_2$As), 124.18, 129.67, 131.40, 133.14, 134.61 (As*Ph*$_3$) ppm.

2.2.4. $[(C_6H_5)_3ECH_3][InX_4]$

2.2.4.1. $E = P$, $X = Br$. InBr (0.41 g, 2.10 mmol) and CH_2Br_2 (0.5 ml, 1.24 g, 7.1 mmol) were stirred in acetonitrile (10 ml) until the InBr dissolved. Volatiles were removed under vacuo, and the product kept under vacuum to ensure removal of excess CH_2Br_2; the resultant oil was redissolved in CH_3CN (10 ml) and $P(C_6H_5)_3$ (0.55 g, 2.10 mmol) added to this solution, which was stirred for 1 h, after which HBr (170 mg, 2.10 mmol, 0.35 ml of 48% aqueous solution) was added and the reaction stirred for 1 h. Volatiles were again removed under vacuum, and the resultant white solid recrystallised in 20 ml of acetone–ethanol (1:1, v/v) to yield $[(C_6H_5)_3PCH_3][InBr_4]$ (0.58 g, 0.81 mmol, 39%) as colorless microcrystals. Anal. Found: In, 15.8; Br, 44.5; Calc. for $C_{19}H_{18}Br_4InP$; In, 16.1; Br, 44.9. ^{1}H-NMR ($CDCl_3$): 7.4–7.9, m, 5H; 2.86, d, JH, $J_{P–H} =$ 13.2 Hz. ^{18}C-NMR ($CDC1_3$); 136.3, d, $J_{P–H}$ 3.0 Hz, aromatic para; 133.7, d, $J_{P–H} = 10.8$ Hz, aromatic ortho; 131.5, d, $J_{P–H} = 13.1$ Hz, aromatic meta; 119.0, d, $J_{P–H} = 89.0$ Hz, aromatic ipso; 11.4, d, $J_{P–H} = 58.7$ Hz, methyl.

2.2.4.2. $E = As$, $X = Br$. $Br_3InCH_2As(C_6H_5)_3$ (0.41 g, 0.61 mmol) was dissolved in acetonitrile (10 ml) and HBr (0.144 g, 1.77 mmol, 0.30 ml of 48% aqueous solution) added. The reaction mixture was stirred for 16 h, and then refluxed for 1.5 h. Removal of all volatiles under vacuum gave an oil, which was dissolved in hot ethanol (10 ml); upon cooling, $[(C_6H_5)_3AsCH_3][InBr_4]$ (0.33 g, 0.44 mmol, 72%) precipitated as yellow needles, which were collected under filtration and dried under vacuo. Anal. Found: In, 14.2; Br, 41.0; Calc. for $C_{19}H_{18}AsBr_4In$; In, 15.2; Br, 42.3 ^{1}H-NMR ($CDCl_3$): 7.6–7.9, m, 5H; 2.81, s, 1H. ^{13}C-NMR ($CDCl_3$): 134.7, aromatic para; 132.0, aromatic ortho; 131.3 aromatic meta; 121.0 aromatic ipso; 9.2 methyl.

$E = As$, $X = I$. $I_3InCH_2AsPh_3$ (1.00 g, 1.22 mmol) and HI (57% in water, 0.16 ml, 0.16 g, 1.22 mmol) were stirred in acetonitrile (20 ml) for 3 h. The resultant yellow precipitate was collected, and the mother liquor concentrated under vacuo to 50% of its initial volume, when crystals of $[(C_6H_5)_3AsCH_3][InI_4]$ (0.61 g, 0.64 mmol, 53%) precipitated. Anal. Found: In, 11.8; I, 52.3; Calc. for $C_{19}H_{18}AsInI_4$; In, 12.2; I, 53.8. ^{1}H-NMR ($CDCl_3$) 7.92–7.77 m, 5 H (C_6H_5), 3.20 s, 1H, CH_3, ppm.

2.2.5. $[(C_6H_5)_3\ SbCH_2Br][InBr_4]$

$Br_3InCH_2Sb(C_6H_5)_3$ (0.30 g, 0.42 mmol) and a 0.5 M solution of Br_2 in CCl_4 (0.83 ml, 0.42 mmol) were stirred together in CH_2Cl_2 (10 ml) at r.t. for 12 h, by which time the red color of the bromine had discharged. Volatiles were removed under vacuum to give a brown solid, which was recrystallised in acetone–ethanol (95%; 1:1, v/v) to yield $[(C_6H_5)_3$-$SbCH_2Br][InBr_4]$ (0.27 g, 0.31 mmol, 74%). Anal. Found: In, 13.5; Br, 45.6; Calc. for $C_{19}H_{17}Br_5InSb$; In, 13.0; Br, 45.3. ^{1}H-NMR (acetone-*d*6) 7.75–7.97, m, 15H; 5.14, s, 2H. ^{13}C-NMR: 136.2; 134.1; 131.2; 123.9; 13.3 ppm.

2.2.6. Attempted reactions with electrophiles

In addition to the reaction with HBr and Br_2 described above, we investigated the possible reactions of the Group 15 adducts of Br_2InCH_2Br with a series of electrophiles (benzyl chloride and bromide, allyl bromide and iodide, trityl bromide, p-chlorobenzaldehyde). No reaction was detected in any of these systems after refluxing for some hours in THF or dioxane, and the X_3InCH_2L compounds ($X = Br$, $L = N(C_2H_5)_3$,

Table 1
Summary of crystal data, intensity collection and structural refinement for compounds **1**–**4**

Compound	**1**	**2**	**3**	**4**
Formula	$C_7H_{17}NInBr_3$	$C_{19}H_{17}AsInBr_3$	$C_{19}H_{17}SbInBr_3$	$C_{19}H_{17}AsInI_3$
fw M_r	469.77	674.80	721.63	815.77
Crystal system	Monoclinic	Orthorhombic	Orthorhombic	Monoclinic
Space group	$P2_1/n$	*Pbca* (No.61)	*Pbca* (No.61)	$P2_{1/n}$
a (Å)	7.362(2)	15.553(7)	15.439 (6)	12.0122(2)
b, (Å)	14.700(2)	21.646(8)	22.016(4)	15.8526(3)
c, (Å)	13.049 (1)	12.920(10)	13.138(5)	13.4180(3)
β (°)	98.90(1)			109.933(1)
V (Å^3)	1395.1(4)	4349.4(3.8)	4465.7(2.3)	2402.04(8)
d_{calc} (g cm^{-3})	2.237	2.06	2.41	2.256
Z	4	8	8	4
Crystal dimensions (mm)	0.2 × 0.2 × 0.2	0.1 × 0.1 × 0.1	0.1 × 0.1 × 0.1	0.1 × 0.1 × 0.1
Absorbtion coefficient (mm^{-1})	10.25	62.35	50.45	6.21
Temperature (°C)	25	23	23	25
Data collection range (2θ) (°)	2.10–28.33	−50	−45	1.97–25.0
Total number of rflections measured	4052	4120	4059	12 103
Number of unique data variables	2535:110	717:77	911:123	4189:122
R	0.0418	0.064	0.062	0.0481
R_w	0.0368	0.054	0.049	0.0431
max Δ/δ in final cycle		0.03	0.01	
ρ_{max} in final difference map (e Å^{-3})	0.98, −0.56	1.36, −0.89	1.61, −0.93	1.80, −0.82

$As(C_6H_5)_3$, $Sb(C_6H_5)_3$; $X = I$, $L = As(C_6H_5)_3$) were recovered at the end of this treatment.

2.3. Crystallographic studies

The procedures for $Br_3InCH_2As(C_6H_5)_3$ (**2**) and $Br_3InCH_2Sb(C_6H_5)_3$ (**3**) were essentially identical. Suitable crystals were mounted on glass fiber and X-ray diffraction data were collected on a Rigaku AFC6S instrument, with graphite monochromated Mo–K$_\alpha$ radiation ($\lambda = 0.71069$ Å). Cell constants and orientation matrices for data collection were obtained using 25 strong reflections in the range of $22.54 < 2\theta < 32.35°$. The space groups were identified from the systematic absences, and confirmed subsequently by the successful structure refinements. Decay and absorption corrections (PSI scan) were applied, and the data were also corrected for Lorentz and polarization effects. The structures were solved by direct methods. For compound **3**, the indium, bromine and antimony atoms were refined anisotropically, and all others isotropically; hydrogen atoms were introduced initially in ideal positions and subsequently refined isotropically. Crystals of compound **2** diffracted poorly, and in order to solve the structure with the available data it was necessary to treat the phenyl rings as units, using the programmed parameters R(C–C) = 1.40 Å and C–C–C = 120°. The programs and other data used are listed in [10–15], and details of the data collection are given in Table 1.

For $Br_3InCH_2N(C_2H_5)$ (**1**) and $I_3InCH_2As(C_6H_5)_3$ (**4**), diffraction data were collected by attaching single crystals to a quartz fiber mounted on a Siemens SMART three-circle diffractometer equipped with graphite-monochromatized Mo–K$_\alpha$ radiation and a CCD area detector, and controlled by a Pentium-based PC running the SMART software package [16]. Omega-scans were used in such a way that an initial 180° scan range consisting of 0.3° intervals was followed by three further 120, 180, and 120° scans with ϕ offsets of 88, 180, and 268°, respectively. This strategy samples the sphere of reciprocal space up to $2\theta = 56.62°$. Cell parameters were refined using the centroid values of 300 reflections with 2θ angles up to 56.62°. Raw frame data were integrated using the SAINT program [17]. The structure was solved by direct methods [18]. An empirical absorption correction was applied to the data using the program SADABS [19]. For compound **4**, only indium, iodine and arsenic atoms were refined anisotropically.

Figs. 1 and 2 show the structures of **1** and **4**; **2** and **3** are essentially isostructural with **4**, as is the

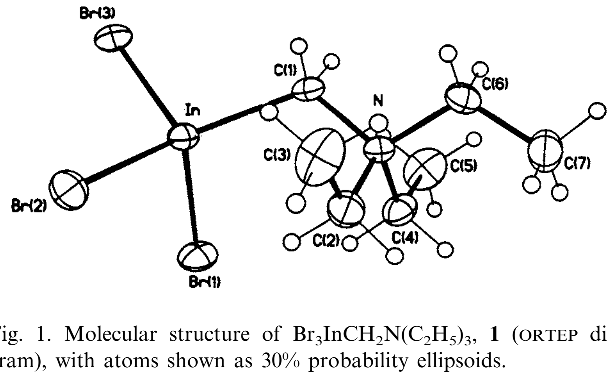

Fig. 1. Molecular structure of $Br_3InCH_2N(C_2H_5)_3$, **1** (ORTEP diagram), with atoms shown as 30% probability ellipsoids.

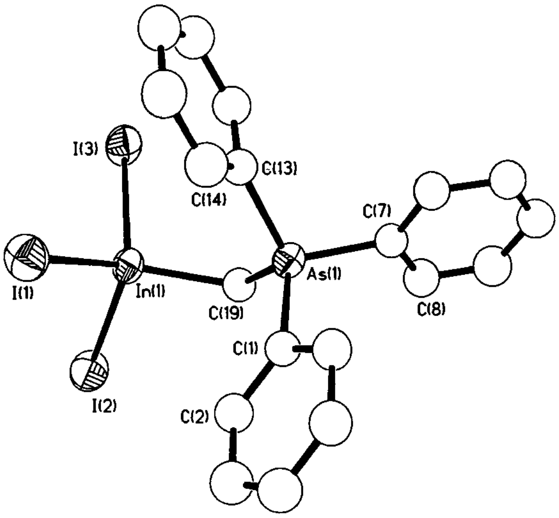

Fig. 2. Molecular structure of $I_3InCH_2As(C_6H_5)_3$, **4**, (ORTEP diagram), with atoms shown as 30% probability ellipsoids. Hydrogen atoms have been omitted for clarity.

Table 3
Calculated total energies (in eV)

	Energy
$Br_3InCH_2N(C_6H_5)_3$ [a,b]	3792.53701, 3792.22379
$Br_3InCH_2P(C_6H_5)_3$ [a,b]	3752.31714, 3751.70850
$Br_3InCH_2As(C_6H_5)_3$ [a,b]	3755.17799, 3754.65526
$Br_3InCH_2Sb(C_6H_5)_3$ [a,b]	3779.81651, 3779.11470
Br_2InCH_2Br [c]	1266.80743
Br_3InCH_2 [c]	1265.90056
$InBr_3$ [c]	1118.18624
$N(C_6H_5)_3$	2524.36436
$P(C_6H_5)_3$	2482.84111
$As(C_6H_5)_3$	2486.62269
$Sb(C_6H_5)_3$	2512.91410
$H_2CN(C_6H_5)_3$	2671.09632
$H_2CP(C_6H_5)_3$	2631.02178
$H_2CAs(C_6H_5)_3$	2633.94666
$H_2CSb(C_6H_5)_3$	2658.06945

[a] See Section 2.
[b] See Section 2.
[c] Values from [9].

triphenylphosphine derivative. The structural data relevant to the present paper are given in Table 2. Complete tables of bond distances and angles, atomic coordinates and thermal parameters are available as supporting information.

2.4. Calculation methods and models

The PM3 semiempirical method [20,21] implemented in the MOPAC (version 5.0) program package [22] was used with standard indium parameters for this procedure. The geometry optimization of the molecules via gradients and minimization of energy were carried out using the BFGS algorithm, which makes use of first and second derivatives. The initial structural parameters for the $Br_3InCH_2E(C_6H_5)_3$ (E = P, As, Sb) models were those determined by X-ray structural studies. There are two entries in Table 3 for the calculated total energy for each adduct. For (a), the structure was allowed to refine freely, but this procedure resulted in models with In–C–E angles of ca. 90°, much smaller than the experimental values (ca. 115–118°); no other significant differences from the experimental values were observed. Procedure (b) gives the total energies obtained by constraining the In–C–E bond angles close to the experimental values, and we consider only those results obtained by this latter procedure in the discussion.

For all the calculated structures, the In–Br bond distances are considerably shorter than the experimental values. This difference is inherent in the PM3 method, and has been discussed earlier [21,22]. The

Table 2
Important bond distances (Å) and angles (°)

	$Br_3InCH_2NEt_3$	$Br_3InCH_2PPh_3$ [a]	$Br_3InCH_2AsPh_3$	$Br_3InCH_2SbPh_3$	$I_3InCH_2AsPh_3$
Bond length					
In–X [b] (av)	2.529(1)	2.512(2)	2.508(6)	2.509(5)	2.724(1)
In–*C*H_2	2.185(5)	2.18(1)	2.17(5)	2.16(3)	2.184(7)
E–*C*H_2 [c]	1.507(6)	1.79(1)	1.97(5)	2.03(3)	1.924(6)
E–C(R) [c](av)	1.519(1)	1.80(1)	1.89(2)	2.14(3)	1.929(7)
Bond angles					
X–In–X [b,d]	105.3(1)[5.1]	106.8(1)[5.2]	106.7(2)[5.5]	106.4[4.3]	108.7(1)[1.5]
X–In–*C*H_2 [b,d]	113.4(2)	112.1(3)[12.0]	112(1) [12]	112.4[5.0]	110.0(2)[14.7]
In–CH_2–E [c]	119.2(4)	118.9(6)	115(2)	118(2)	119.8(3)
CH_2–E–C(R) [c,d]	109.9(4)[1.7]	110.1(5)[1.9]	111(1) [3]	110(1)[1]	110.2(3)[2.2]
C(R)–E–C(R) [c,d]	109.0(4)[4.8]	108.8(6)[2.0]	108(1) [3]	108(1)[3]	108.0(3)[2.9]

[a] Results from [3].
[b] X = Br, I.
[c] E = N, P, As, Sb.
[d] Parentheses indicate typical experimental uncertainty; value in square brackets is the difference between highest and lowest values.

reasons for the effect are not clear, but two relevant factors are (i) the exchange and coulombic integrals at the zero differential overlap approximation are excluded, and (ii) the method considers only indium s- and p-orbitals, and so neglects any contributions from metal d-orbitals, which may be important in the stabilisation of these molecules.

3. Results and discussion

3.1. Structural results

The four molecules whose structures are reported here have a number of important features in common with each other, and with the previously reported $Br_3InCH_2P(C_6H_5)_3$ [3]. The summary of bond angles in Table 2 shows that the stereochemistry at indium and at the Group 15 atom is distorted tetrahedral in both cases. The In–CH_2–E angles are also reasonably constant in all five molecules, at 118 ± 2°, and the bond distances are in keeping with these consistencies. In particular, the In–CH$_2$ length of 2.18 ± 0.01 Å is essentially constant, and in agreement with previous results for adducts for Br_2InCH_2Br [3,9], but lower than in In–$(CH_2)_n$–In compounds [23,24]. The E–CH_2 bond distances show a dependence on E, which is discussed below.

The r(In–Br) distances in the three triphenyl derivatives are constant within the experimental uncertainty, and close to the value of 2.518 Å (av) found for the anion $Br_3InCH_2Br^-$, but significantly lower than in the neutral adduct $Br_2(THF)_2In(CH_2)In(THF)_2Br_2$ (r(In–Br) = 2.517(1), 2.544(1) Å) [23] and the corresponding anion $[Br_3In(CH_2)_4InBr_3]^{2-}$ (r(In–Br) = 2.543(3) Å (av)) [24]. There is little difference between the structures of $Br_3InCH_2As(C_6H_5)_3$ and $I_3InCH_2As(C_6H_5)_3$, apart from the indium–halogen values.

Table 4
Calculated HOMO and LUMO energy levels (in eV)

Structure	HOMO	LUMO
$Br_3InCH_2N(C_6H_5)_3$	−11.590	−3.630
$Br_3InCH_2P(C_6H_5)_3$	−13.556	−5.155
$Br_3InCH_2As(C_6H_5)_3$	−10.318	−1.486
$Br_3InCH_2Sb(C_6H_5)_3$	−9.906	−1.270
Br_2InCH_2Br [a]	−9.009	−1.811
Br_3InCH_2 [a]	−10.520	−3.825

[a] Values from [9].

Table 5
Calculated bond distances (Å), bond angles (°), and bond orders, for $Br_3InCH_2E(C_6H_5)_3$ (E = N, P, As, Sb)

	N	P	As	Sb
Bond length				
In–C	2.18	2.16	2.16	2.14
E–CH_2	1.50	1.72	1.83	2.18
E–C_{ar}	1.52	1.76	1.87	2.12
In–Br_a	2.18	2.20	2.20	2.19
Bond angles				
InCH$_2$	112.7	120.1	112.1	116.2
Br–In–CH$_2$	111.5	112.6	112.3	110.9
H$_2$$C$E–$C_{ar}$	110.0	111.1	110.7	112.0
Bond orders				
In–E	0.89	0.89	0.90	0.90
In–CH$_2$	0.91	0.91	0.89	0.91
E–CH$_2$	0.98	0.91	0.95	0.69
E–C_{ar} [a]	0.95	0.83	0.86	0.77

[a] Mean value.

3.2. Quantum mechanical calculations

Table 3 gives the calculated total energies of the four molecules $Br_3InCH_2E(C_6H_5)$, including the hypothetical E = N species, and for various related molecules. The two sets of values for the adducts refer to the different methods of calculation described in Section 2.4. Table 4 presents the calculated energy levels for the HOMO and LUMO orbitals in the adducts. The results in Table 3 lead to calculated ΔE_r values for adduct formation, by the process

$$Br_2InCH_2Br + E(C_6H_5) \rightarrow Br_3InCH_2E(C_6H_5)_3 \tag{1}$$

of N = −1.052, P = −2.060, As = −1.225 and Sb = +0.607 eV, or −101, −198, −118 and +59 kJ mol^{-1}. The value for the nitrogen system predicts that a stable ylid $Br_3InCH_2N(C_6H_5)_3$ should be accessible; in fact this compound could not be obtained, which may reflect the steric crowding at N in triphenylamine, since the analogous triethylamine compounds has been prepared. Equally, the formation of the $Sb(C_6H_5)_3$ adduct is predicted to be endothermic, whereas the compound is in fact stable. The calculated energies for Eq. (1) are probably at the limit of the reliability of the calculations, so that conclusions based on small differences between large values are not reliable. On the other hand, the calculated bond lengths and angles, calculated net atomic charges, bond orders and atomic orbital populations are given in Tables 5 and 6, and the agreement between the values in Table 5 and the experimental values in Table 2 is satisfying. The differences in bond lengths and angles are below 5%, except for the In–Br distances, which seems to be an inherent difficulty in this method (see above). The good fit speaks to the reliability of the calculated parameters.

One very significant feature of the $Br_3InCH_2E(C_6H_5)_3$ structures is the calculated charge distribution (Table 6), which reveals a considerable negative charge at the carbon atom bonded to the metallic center (as high as −0.6 for the phosphorus and arsenic compounds), and

Table 6
Atomic orbital electron populations and net atomic charges in $Br_3InCH_2E(C_6H_5)_3$ (E = N, P, As, Sb)

Populations	N	P	As	Sb
Atom (orbital)				
In(s)	0.913	0.919	0.913	0.924
In(p_x)	0.750	0.741	0.728	0.743
In(p_y)	0.680	0.669	0.673	0.677
In(p_z)	0.638	0.621	0.617	0.635
C(s)	1.221	1.222	1.221	1.231
C(p_x)	1.106	1.136	1.112	0.980
C(p_y)	0.924	1.107	1.119	0.805
C(p_z)	1.118	1.125	1.118	1.062
E(s)	1.176	1.222	1.183	1.836
E(p_x)	0.942	0.621	0.700	0.771
E(p_y)	0.998	0.658	0.721	0.864
E(p_z)	0.939	0.599	0.665	0.757
Net Charges				
Br [a]	−0.30	−0.31	−0.30	−0.30
In	0.02	0.05	0.07	0.02
C	−0.37	−0.59	−0.57	−0.08
E	0.94	1.90	1.73	0.77
H(CH_2) [a]	0.14	0.15	0.15	0.11
C_{ar} [a,b]	−0.10	−0.14	−0.13	−0.10
H_{ar} [a,b]	0.13	0.11	0.12	0.12

[a] Mean value.

[b] ar = aromatic.

Table 7
^1H- and ^{13}C-NMR chemical shifts (ppm; $Me_4Si = 0$) and net atomic charges of the methylene group in $Br_3InCH_2E(C_6H_5)_3$ and $Br_2In(L)_nCH_2Br$ compounds

Compound	Net atomic charge	^1H	^{13}C
$Br_3InCH_2P(C_6H_5)_3$ [a]	−0.59	2.30	10.20
$Br_3InCH_2As(C_6H_5)_3$ [b]	−0.57	2.21	9.58
$Br_3InCH_2Sb(C_6H_5)_3$ [b]	−0.08	2.83	nd [f]
$Br_2In(Et_2O)_{1/2}CH_2Br$ [c,d]	nc [e]	3.07	17.6
$Br_2In(diox)_2CH_2Br$ [a,d]	−0.07	2.77	18.96
$[Br_3InCH_2Br]^-$ [a,d]	−0.01	2.75	18.30

[a] In CD_3CN.

[b] In $(CD_3)_2CO$.

[c] NMR spectra in CD_2Cl_2 solution.

[d] Results from [9].

[e] nc, not calculated.

[f] nd, not detected.

the increased positive electron density at the heteroatom E, all of which establishes unequivocally the presence of the ylid $H_2C^{\delta-}$–$^{\delta+}X(C_6H_5)_3$ in the $Br_3InCH_2E(C_6H_5)_3$ structures. This is a particularly interesting conclusion when one considers that the organoindium ylids are formed from a starting material, Br_2InCH_2Br, in which a great deal of positive charge is situated on the carbon atom, $Br_3In^{\delta-}$–$^{\delta+}CH_2$, in one tautomeric form.

The formation of the free ylids, $H_2C^{\delta-}$–$^{\delta+}E(C_6H_5)_3$, from the organoindium complex is not an easy process. The calculated energies in Table 3 allow ΔE to be derived for the processes

$$Br_3InCH_2E(C_6H_5)_3 \rightarrow InBr_3 + H_2C^{\delta-}\text{–}^{\delta+}E(C_6H_5)_3 \quad (2)$$

For E = P, $\Delta E = 2.500$, As = 2.522, and Sb = 2.859 (in eV), or 241, 243 and 276 kJ mol^{-1}, which suggests that decomposition will only occur at high temperatures, as indeed was observed in the TGA experiments (see below), in which decomposition was detected above 170°C for all three species. The data further imply that free ylids are unlikely to be involved as readily accessible intermediates in reactions starting with the $Br_3InCH_2E(C_6H_5)_3$ compounds.

3.3. Spectroscopic results

The NMR results for the CH_2 protons in the $Br_3InCH_2E(C_6H_5)_3$ compounds are collected together in Table 7, and compared with the calculated atomic charge at the carbon atom in question; results are also shown for the ether, 1,4-dioxane and bromide derivatives of Br_2InCH_2Br, in which the ligand is known to be bonded to the indium atom [9]. There is a clear relationship between the observed ^1H chemical shift and the net atomic charge at the methylene carbon atom in the $E(C_6H_5)_3$ derivatives, so that for E = As and Sb, the resonances at 2.21 and 2.83 ppm reflect the higher electronic density at the carbon of the arsenic derivative. Equally, the antimony compound, in which the atomic charge on the methylene carbon is similar to those in the ether, dioxane and bromide adducts, shows a proton resonance close to that in to these compounds, and $Br_3InCH_2SC(NMe_2)_2$ and the triphenylarsenic adduct have similar chemical shifts (2.44 ppm [3,8]) and structures. We were not able to detect the carbon resonance of the antimony derivative. This is a common problem in organoindium compounds, in which there is believed to be strong coupling with the indium atom (I = 9/2), and in addition antimony itself has two high-spin isotopes (^{121}Sb, I = 5/2 and ^{123}Sb, I = 7/2). The ^{13}C resonances of the methylene group of the phosphorus and arsenic derivatives, at 10.20 and 9.58 ppm, are at considerably higher field than that in the parent molecule Br_2InCH_2Br. 1/2 Et_2O (17.6 ppm) [3], again agreeing with the increased electron density at the methylene carbon of the $Br_3InCH_2E(C_6H_5)_3$ compounds, as predicted by the calculations.

3.4. Mass spectra and thermal decomposition

The E.I. mass spectra of the $Br_3InCH_2E(C_6H_5)_3$ compounds are given in Table 8. No molecular ions were detected, but the fragment $[Br_2InCH_2E(C_6H_5)_3]^+$ resulting from the rupture of one indium–bromine bond was observed in each case, as was the ylid $[H_2C{=}E(C_6H_5)_3]^+$, which results from the fission of the indium–carbon bond

$$BrInCH_2E(C_6H_5)_3 \rightarrow Br_3In + [CH_2{=}E(C_6H_5)_3]^+ \quad (3)$$

Additional observed fragments are all derived from the $[CH_2 = E(C_6H_5)_3]^+$ylid, and include $[E(C_6H_5)_3]^+$, $[E(C_6H_5)_2]^+$, $[E(C_6H_5)]^+$, $[H_5C_6{-}C_6H_5]^+$, and $[C_6H_5]^+$ .The TGA curves, showing weight loss as a function of temperature, were obtained for all the $Br_3InCH_2E(C_6H_5)_3$ compounds. Fig. 3 depicts the result for the arsenic compound, which is the best behaved example. There are three separate stages of weight loss, over the temperature ranges 178–326°C (14.5% loss), 326–453°C (63.7% loss), and finally an 11.8% loss at 453–552°C. The residual mass is equal to 10.0% of the initial quantity of adduct. The first stage corresponds to loss of CH_2 and C_6H_5 groups (calc 13.5%), and that of 63.7% to the removal of $InBr_3$ and a second C_6H_5 group (calc. 63.5%); the loss of 11.8% corresponds to removal of the third C_6H_5 group (calc 11.4%), and the final residue of 10.0% is assigned to elemental arsenic (calc. 10.0%).

The thermal decomposition pathway, together with the fragmentation pattern in the mass spectrum of $Br_3InCH_2As(C_6H_5)_3$ suggests the thermal decomposition mechanism:

$$Br_3InCH_2As(C_6H_5)_{3(s,1)} \rightarrow Br_3In_{(s,1)} + H_2C{=}As(C_6H_5)_{3(s,1)} \quad (4)$$

$$H_2C{=}As(C_6H_5)_{3(s,1)} \rightarrow As(C_6H_5)_{2(s,1)} + 1/n(CH_2)_{n(g)} + 1/2(C_6H_5)_{2(g)} \quad (5)$$

$$As(C_6H_5)_{2(s,1)} \rightarrow As(C_6H_5)_{(s,1)} + 1/2(C_6H_5)_{2(g)} \quad (6)$$

Table 8
Mass spectrometric results: *m*/*e*, with relative abundances (%) in parentheses, for $Br_3InCH_3E(C_6H_5)_3(E = P, As, Sb)$

Fragment	P	As	Sb
$[Br_2InCH_2E(C_6H_5)_3]^+$	549(4.6)–551(8.0)–553(3.8)	593(7.1)–595(12.8)–597(4.4)	639(0.8)–641(1.9)–643(1.9)–645(0.8)
$[H_2C{=}E(C_6H_5)_3]^+$	276(44.6)	320(35.2)	366(8.3)–368(6.00)
$[HC{=}E(C_6H_5)_3^+$ or $H_2C{=}E(C_6H_5)_2C_6H_4]^+$	275(100)	319(80.9)	365(13.3)–367(11.9)
$[E(C_6H_5)_3]^+$	262(9.5)	306(29.1)	352(8.3)–354(6.5)
$[(EC_6H_5)_2]^+$	185(11.9)	229(15.6)	275(19.9)–277(8.0)
$[E(C_6H_5)]^+$	183(42.6)	227(56.8)	273(21.1)
$[E(C_6H_5)]^+$	nd [a]	152(100)	198(100)–200(66.3)
$[(C_6H_5)_2]^+$	nd [a]	154(10.0)	154(50.7)
$[C_6H_5]^+$	77(6.4)	77(1.4)	77(17.5)

[a] nd = not detected.

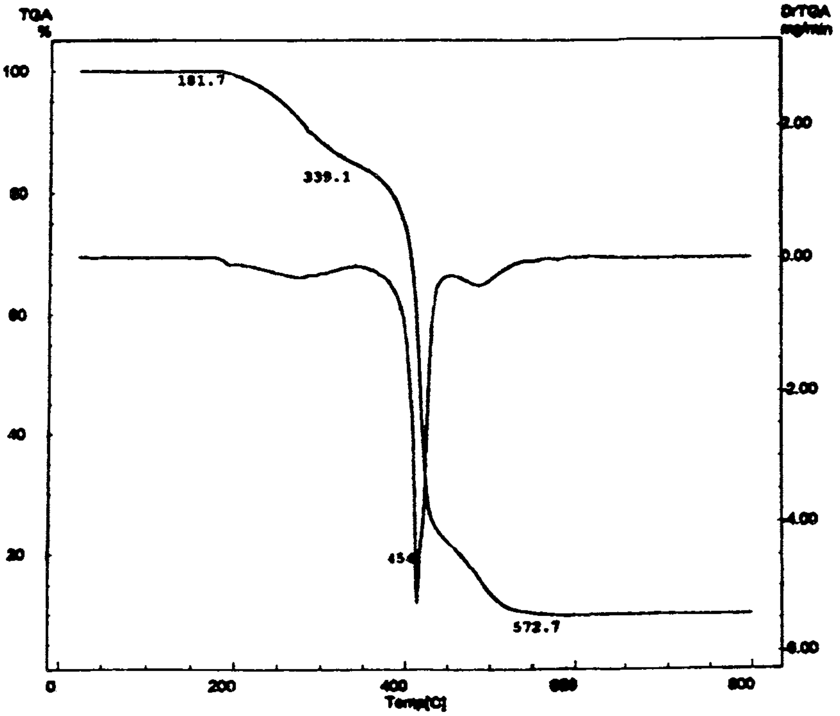

Fig. 3. TGA curve for $Br_3InCH_2As(C_6H_5)_3$.

$$As(C_6H_5)_{(s,l)} \rightarrow As + 1/2(C_6H_5)_{2(g)} \quad (7)$$

3.5. Preparative and mechanistic aspects

The Group 15 ylids $CH_2E(C_6H_5)_3$, are strong nucleophiles, and are known to react with suitable electron pair acceptors, and we therefore studied the reaction of the organoindium ylids with the simplest electrophile, namely the proton, in order to verify the possibility of using these complexes as ylid sources. We were successful in preparing the $[CH_3E(C_5H_6)_3][InBr_4]$ salts for E = P, As, by the process

$$Br_3InCH_2E(C_6H_5) + HBr \rightarrow [CH_3E(C_6H_5)_3]\ [InBr_4] \quad (8)$$

The onium salts were characterised by elemental analysis and NMR spectroscopy (see Section 2); the spectrum of the phosphorus derivative compares well with an authentic sample of the triphenylmethylphosphonium cation, including the P–H coupling constants reported as 88.6 (ipso), 10.7 (ortho), 12.9 (meta), 3.0 (para) and 57.1 Hz (methyl) [23]. The compound $I_3InCH_2As(C_6H_5)_3$ undergoes a reaction similar to Eq. (8).

The antimony derivative does not react with HBr under the conditions used succesfully for the phosphorus and arsenic analogues, but the reaction of $Br_3InCH_2Sb(C_6H_5)_3$ with bromine gave the addition product formulated as $[(C_6H_5)_3SbCH_2Br][InBr_4]$. The NMR spectrum of this product (Section 2) shows the Sb–CH_2–Br resonances at 5.14 ppm (^1H) and 13.3 ppm (^{13}C); there is a considerate shift downfield for the methylene protons, compared to the parent molecule (2.83 ppm), consistent with the formation of the stibonium cation$[BrCH_2Sb(C_6H_5)_3]^+$ by the reaction

$$Br_3InCH_2(C_6H_5)_3 + Br_2 \rightarrow [BrCH_2Sb(C_6H_5)_3][InBr_4] \quad (9)$$

These reactions with HBr and Br_2 were the only successful results in the attempts at reacting $Br_3InCH_2E(C_6H_5)_3$ adducts with electrophiles. There are two ways of understanding these results. The first is to consider the high energies associated with Eq. (2); for all three adducts, the formation of the appropriate ylid is highly endoergic, in agreement with the thermogravimetric results, so that the energetics of a reaction between the adduct and an electrophile are thermodynamically unfavourable. The second approach is to consider the charge distribution in the $InCh_2E$ core of the adducts, using the results in Table 6. For the phosphorus compound, for example, one has Scheme 2 with a considerable degree of negative charge on the carbon atom, and a large positive charge on phosphorus, so that the carbon is surrounded by four positive centers which will inhibit attack by large electrophiles at this atom. With HBr, the cleavage of the In–CH_2E bond is in agreement with the known chemistry of organoindium compounds, and in this the small electrophile (H^+) in the highly polar HBr molecule interacts favorably with the In–C bond. The absence of a reaction between HBr and the antimony ylid can be correlated with the near lack of polarity in the In–C bond in this latter molecule (see Table 6). These examples apart, attack on $Br_3InCH_2E(C_6H_5)_3$ by bulky electophiles will be hindered sterochemically, as well as being energetically unfavorable.

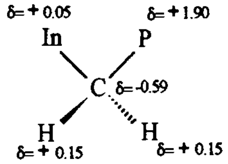

Scheme 2.

4. Conclusions

The α-halogeno-indium carbenoids, of general structure $X_2InCR^1R^2X$ are of considerable interest in organic synthesis. The results described here and elsewhere clearly characterise two electron deficient sites in these compounds, namely the metal center and the carbon atom. The lack of electron density at the carbon is a result of a strong interaction between the halogen and the metallic center (Scheme 3) and the ultimate result of halide transfer is the tautomeric structure IB, which has an electrophilic carbene group.

Reaction with a series of selected ligands, L gives organoindium ylids of the general structure, $X_3InCR^1R^2L$, particularly when L is ligand capable of accommodating a positive charge, such as amine, phosphine, arsine, stibine, etc. and one result of this process is therefore an unpollung of the carbene from the initial electrophilic $X_2InCR^1R^2X$ compound to the final nucleophilic organoindium ylid $X_3InCR^1R^2L$. Calculations in this and earlier work confirm these effects, and equally provide a rationale for the spectroscopic properties of these ylids, for their thermal decomposition reactions, and for the lack of reactivity with bulky electrophiles.

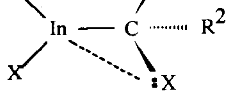

Scheme 3.

Acknowledgements

This work was supported in part by Operating Grants (to C.P.) form the Conselho Nacional de Desenvolvimento Cientifico e Tecnologico — CNPq CAPES and PAPESQ — PB Borazil). Two of us (L.A.F. and R.K.K) thank the CNPq for the award of scholarships (PIBIC-UFPb program). Support from the Natural Sciences and Engineering Research Council of Canada (to D.G.T.) is also acknowledged. We thank Professor D.W. Stephan and Dr Glenn Yap (University of Windsor) for the X-ray crystallographic studies of compounds **1** and **4**.

References

[1] S. Araki, Y. Butsugan, J. Chem. Soc., Chem. Commun. (1989) 1286

[2] S. Araki, T. Hirashita, K. Shimizu, K.T. Ikeda, Y. Butsugan, Tetrahedron 52 (1996) 2803.

[3] T.A. Annan, D.G. Tuck, M.A. Khan, C. Peppe, Organometallics 10 (1991) 2159.

[4] J.E. Santos, C. Peppe, M.A. Brown, D.G. Tuck, Organometallics 15 (1996) 2201.

[5] L.N.H. Arakaki, M.Sc. thesis, Universidade Federal da Paraiba, Brazil.

[6] C. Peppe, D.G. Tuck, unpublished results.

[7] J.A. Nobrega, C. Peppe, Z. Tian, M.A. Brown, D.G. Tuck, unpublished results.

[8] A.C. Souza, C. Peppe, Z. Tian, M.A. Brown, D.G. Tuck, Organometallics 12 (1993) 3354.

[9] A.B. de Carvalho, M.A.M.A. de Maurera, I.A. Nobrega, C. Peppe, M.A. Brown, D.G. Tuck, M.Z. Hernandes, E. Longo, F.R. Sensato, Organometallics 18 (1999) 99.

[10] C.J. Gilmore, J. Appl. Crystallogr. 17 (1984) 42 MITHRIL.

[11] P.T. Beurskens, DIRDIF. Technical Report, 1, Crystallography Laboratory, Nijmegen, Netherlands, 1984, p. 1984.

[12] International Tables for X-ray Crystallography, Kynock Press, Birmingham, UK, 1974. Tables 2.2A, 2.3.1.

[13] J.A. Ibers, W.C. Hamilton, Acta Crystallogr. 17 (1964) 781.

[14] TEXAN-TEXRAY Structure Analytical Package; Molecular Structure Corp. Houston, TX, 1985.

[15] C.K. Johnson, ORTEP II. Report ORNL-5138, Oak Ridge National Laboratory, Oak Ridge, TN, 1976.

[16] SMART: Data Collection Software, Version 4.050; Siemens Analytical X-ray Instruments Inc.: Madison, WI, 1996.

[17] SAINT: Data Reduction Software, Version 4.050; Siemens Analytical X-ray Instruments Inc. Madison, WI, 1996.

[18] SHELTXL 5.04/VMS: An Integrated System for Solving, Refining and Displaying Crystal Structures from Diffraction Data; Siemens Analytical X-ray Instruments Inc. Madison WI, 1995.

[19] G.M. Sheldrick, SADABS: Empirical Absorption Correction Program, University of Gottingen, Gottingen, Germany, 1996.

[20] J.P.P. Stewart, J. Compt. Chem. 10 (1989) 209.

[21] J.P.P. Stewart, Method J. Compt. Chem. 10 (1989) 221.

[22] J.P.P. Stewart, Quantum Chem. Prog. Exch. Bull 3 (1983) 43.

[23] M. Tschinkl, A. Schier, J. Riede, E. Schmidt, G.P. Gabbai, Organometallics 16 (1997) 4759.

[24] M.A. Khan, D.G. Tuck, Acta Crystallogr. Sect. B. Struct. Sci. B38 (1982) 803.